

Predictive quantum theory of current and optical emission in quantum cascade lasers

T. Kubis^{a*}, P. Vogl^a

^a Walter Schottky Institute, Technische Universität München, Am Coulombwall 3, 85748 Garching, Germany

ABSTRACT

We have implemented a self-consistent non-equilibrium Green's functions approach for vertical charge transport and optical gain in terahertz quantum cascade lasers (THz-QCL) in the stationary limit. We present theoretical results of the current-voltage characteristics and the temperature dependence of the optical gain for GaAs/Al_{0.15}Ga_{0.85}As THz-QCLs and compare our results with experimental data. We find excellent quantitative agreement for the current-voltage characteristics and the peak gain energy and identify non-radiative transitions between the laser levels as primary factor that limits the maximum operation temperature. Furthermore, we find significant coherent leakage of electrons in the upper laser level that increases the threshold current density. We propose a broadening of the collector well to efficiently suppress this coherent leakage and to reduce the threshold current.

Keywords: Quantum transport, Quantum cascade lasers

1. INTRODUCTION

Carrier confinement, coherent tunneling and quantum interference effects as well as incoherent scattering play a crucial role for charge transport in multi-quantum well structures such as terahertz quantum cascade lasers (THz-QCL). Keldysh [1], Kadanoff and Baym [2] have developed the non-equilibrium Green's function theory (NEGF) in the 1960's. This method has been demonstrated to describe quantum transport with scattering accurately [3-11].

Several published implementations of the NEGF method to QCLs invoke a Wannier-Stark basis that incorporates the electric field within the basis [9-11]. This reduces the computational effort to a few QCL periods, but limits the predictability and accuracy in several ways. The structures are assumed to be strictly field periodic. This is only valid if the barriers are sufficiently high, and efficient energy dissipation limits the spatial extension of all included electronic states. Carriers with high kinetic energies and wave functions extending across several periodicity lengths may not be taken into account. Since this approach lies outside the framework of scattering theory for open systems, current conservation cannot be obeyed rigorously.

In this paper, we present results of a NEGF scheme that is applicable to any type of open quantum device connected to equilibrium leads. This scheme allows one to compute transport in devices irrespective of the type and strength of scattering and bias. This method is equally applicable to ballistic or diffusive transport. The electronic states and the state occupancies are calculated self-consistently with one another which guarantees current conservation and the state occupancy according to Pauli's principle. Nonlocal scattering with phonons, charged impurities and rough interfaces is taken into account. The optical gain is calculated in terms of the linear response formalism, based on the self-consistently calculated Green's functions.

We apply this method to a class of THz-QCLs that have been successfully fabricated [12]. Based on our theoretical findings, we propose an optimized structure for the QCL that suppresses coherent leakage and significantly reduces the threshold current. We identify thermal backfilling into the lower laser level and phonon mediated transitions from the upper to the lower laser level as mechanisms that reduce the occupation inversion and limit the maximum operating temperature.

*) Email: kubis@wsi.tum.de, Tel: +498928912762, Fax: +498928912737

2. METHOD

In this paper, we consider laterally homogeneous GaAs/Al_{0.15}Ga_{0.85}As quantum cascade structures. They are in contact with two equilibrium reservoirs at $z = 0$ and $z = L$. The electrons are described within a one-band model with a variable effective mass $m^*(z)$. We use the non-equilibrium Green's function method (NEGF) to calculate stationary electronic transport and optical gain up to the threshold current in THz-QCLs.

We have implemented the Dyson and the Keldysh equations in a real space basis. All Green's functions and scattering self energies are functions of two spatial coordinates z, z' , the lateral momentum k_{\parallel} , and the energy E . The self energies are calculated self-consistently with the Green's functions so that scattering states and transition probabilities between them are self-consistently calculated with the state occupations. Once the Green's functions and self energies have been calculated, observables such as the current and the electron density can be calculated straightforwardly [3,4].

We take into account inelastic acoustic and polar-optical phonon scattering, scattering by charged impurities, interface roughness, and by electron-electron interaction in the Hartree approximation. The full nonlocal momentum and energy dependence of the phonon, impurity and interface roughness self-energies are taken into account. All self energies are calculated in the self-consistent Born approximation to guarantee current conservation exactly. The interface roughness is characterized with a Gaussian in-plane correlation with a correlation length of 8 nm and a roughness step height of ± 1 monolayer in growth direction, i.e. 0.6 nm. These values lie well within the range of typical experimental values for GaAs/AlAs interfaces [13-15]. All remaining material and transport parameters, such as electron-phonon and impurity interaction parameters have been taken from Ref. [16]. The Poisson equation is solved self-consistently with the Green's functions under the condition of global charge neutrality. This requires the slope of the electrostatic potential to be equal at both boundaries. The value of this slope is determined such that the potential drop across the entire device matches the externally applied bias voltage.

We consider charge transport as a scattering problem from source to drain with the QCL structure as the active device. In order to reduce the computational effort, we assume the two semi-infinite leads to consist of field-free QCL periods that remain in thermal equilibrium. The difference in the chemical potentials of the leads defines the applied bias voltage in the device. The electrons enter the device in propagating eigenstates of the respective infinitely extended lead Hamiltonians. Then, the active device can be restricted to a few QCL periods while the electronic and optical properties are still faithfully mimicked.

Our calculations show that for the type of THz-QCLs considered in this paper, it actually suffices to treat a single QCL period as active device. In addition, even a flat band model for the leads (instead of multi quantum wells) yield virtually identical results for voltages up to the threshold voltage. This is a consequence of the high barriers within each QCL period that act as efficient energy filter so that the current does not depend critically on the density of states of the incoming carriers [17].

We calculate the optical absorption coefficient in linear optical response, taking into account the calculated laser states and non-equilibrium state occupations, but we ignore vertex corrections to the self energies. Banit *et al.* has shown [18] that the neglect of vertex corrections overestimates the emission line widths significantly. However, absorption peak positions and zeroes of the absorption coefficient seem to be much less sensitive to this approximation. We define the threshold voltage to be that voltage where the absorption coefficient at the peak gain energy (averaged over the active device) changes sign.

3. RESULTS

We have applied our method for carrier transport and optical gain within the active region of the THz GaAs/Al_{0.15}Ga_{0.85}As QCL structure of Ref. [12]. The geometry of this structure can be symbolically denoted by (30) 92 (55) 80 (27) 66 (41) 155. All quantities are given in Å, the values in parentheses indicate Al_{0.15}Ga_{0.85}As barrier widths, and the underlined value indicates the doped regions of the device. In this example, there is only a single n-doped well with $n = 1.25 \times 10^{16} \text{ cm}^{-3}$. A schematic of the structure is given in Fig. 1 (a). It has been shown in the literature that the lattice temperature of a THz-QCL operated in pulsed mode increases by approximately 20-50 K above the heat sink temperature of 5 K [19, 20]. Therefore, if not stated otherwise, we have set the temperature of the phonon bath and the contact reservoirs to 40 K.

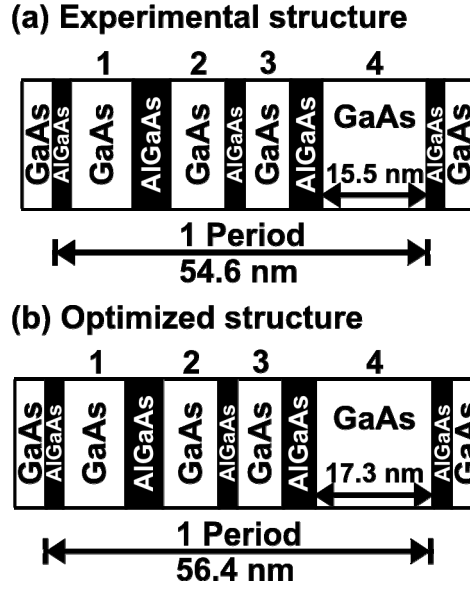


Fig. 1 (a): Schematic diagram of the THz-QCL structure, fabricated and studied experimentally in Ref. [12]. The GaAs quantum wells are numbered for later reference in the main text. Quantum well 1 is the closest to the source. The collector well (#4) is 15.5 nm wide. (b): Schematic diagram of an optimized structure, proposed in this work. The collector well (#4) width has been increased to 17.3 nm.

3.1 Realistic incoherent transport

Iotti and Rossi have shown that incoherent scattering mechanisms are crucial for the transport characteristics of QCLs [21]. Fig. 2 (a) shows a comparison of the measured (dots) and calculated (solid) I-V characteristics of the THz QCL of [12]. Our model excellently reproduces the experimental I-V characteristic which suggests that the implementation of incoherent scattering with phonons, impurities and rough interfaces captures all relevant relaxation mechanisms.

The misalignment of the laser states for voltages above the threshold voltage of approximately 46 mV yields a negative differential resistivity. Here, the coupling of the carriers to the laser field and heating becomes relevant that is not taken into account in the present calculations.

3.2 Coherent leakage

A major portion of the total current stems from coherent transport, as can be deduced from the ballistic calculation depicted in Fig. 2 (a). In fact, the ballistic current amounts to approximately 60% of the experimental current near the threshold voltage.

In order to further illustrate this finding, Fig. 3 (a) depicts the energy and spatially resolved density $n(z, E)$ at 50 mV applied bias. This quantity can be expressed in terms of the lesser Green's functions $G^<$ by the equation

$$n(z, E) = 2 \operatorname{Im} \int d^2 k_{\parallel} G^<(z, z, k_{\parallel}, E) / (2\pi)^3 .$$

One can deduce the occupation inversion from Fig. 3 (a) by noting that the upper and lower laser levels lie at ~ 9 meV and ~ -4 meV (cf. Fig. 4 (a)), respectively. The upper level is occupied in quantum wells #2 and #3 whereas the lower level is practically empty. Most of the electrons do not emit phonons until they reach the widest quantum well #4. The efficiency of coherent tunneling out of the upper laser level into the collector well #4 can be seen from the peaks near the energy of 9 meV in the latter well.

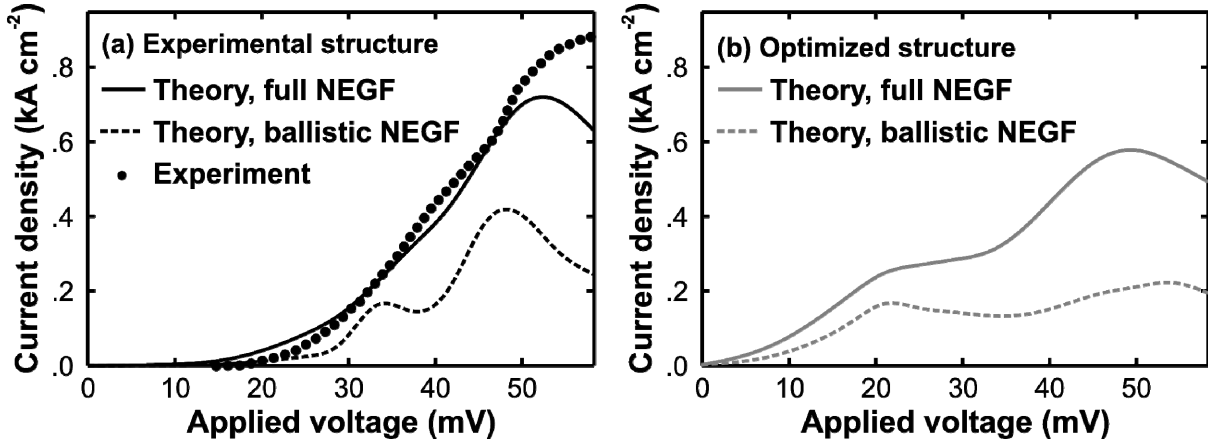


Fig. 2. (a) Experimental (dots) and theoretically predicted (lines) I - V characteristics of the QCL of Fig. 1(a). Calculations that include all incoherent scattering mechanisms (solid) agree well with experiment. In contrast, purely coherent transport (dashed) can only partly reproduce the experiment. (b) Predicted I - V characteristics of the optimized QCL as depicted in Fig 1(b). In contrast to the structure in Fig. 1(a), the ballistic current density (dashed) close to threshold is suppressed.

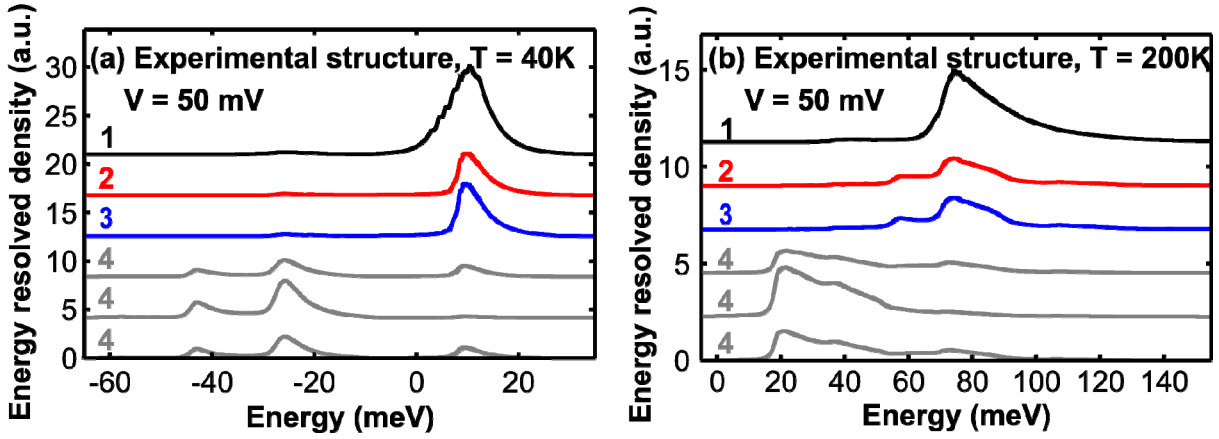


Fig. 3 (a): Energy resolved density $n(z, E)$ in the four numbered quantum wells of the QCL in Fig. 1 (a) at 50 mV bias and a temperature of 40 K. The zero in energy marks the chemical potential of the source. (b) Same as in (a), but the temperature is 200 K.

The mechanism that allows for this dissipation-less transport is illustrated in Fig. 4 (a). It depicts the energy and spatially resolved spectral function $A(z, E)$ of the QCL in Fig. 3 (a) for vanishing lateral momentum $k_{\parallel} = 0$, where

$$A(z, E) = -i [G^R(z, z', 0, E) - G^{R\dagger}(z, z', 0, E)].$$

Here, G^R is the retarded Green's function. The maxima of the spectral function represent resonant states. Both the upper and the lower laser level show up in this figure in the wells #2 and #3. The upper laser level ($E \sim 9$ meV) is aligned with an injecting state in well #1 and gets coherently filled. The lower laser level ($E \sim -4$ meV) is aligned with the second state in the collector well #4 and gets coherently emptied. In addition, the collector state also overlaps with the upper laser level as can be deduced from the small peak marked by the arrow. In spite of being small, this overlap leads to a coherent leakage and reduces the occupation inversion.

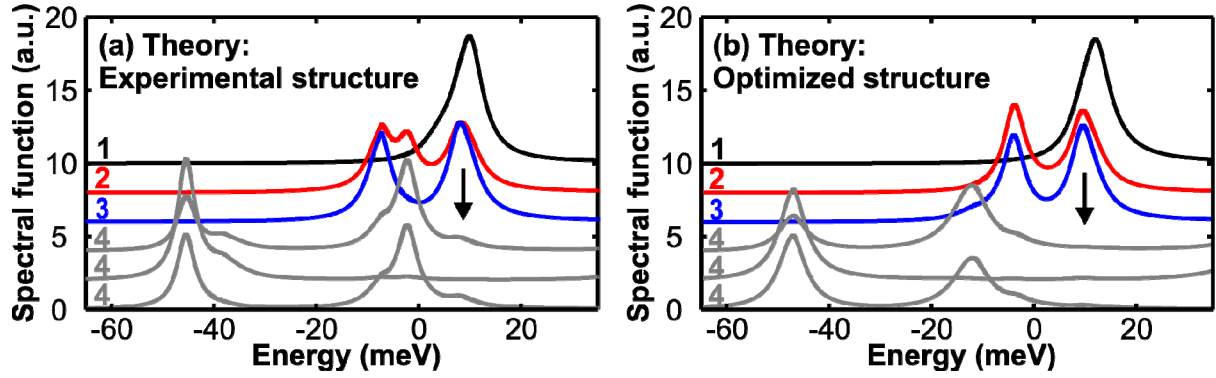


Fig. 4. (a) Spectral function as a function of energy E in the four numbered quantum wells of the QCL in Fig. 1 (a). The second resonance of the collector well ($E = -4$ meV) overlaps with the upper laser level ($E = 9$ meV). This is marked by the arrow. (b) Same as (a) but in the four numbered quantum wells of the QCL in Fig. 1 (b). In contrast to (a), the second collector well state does not overlap with the upper laser level.

3.3 Optimized structure

The coherent leakage of the QCL structure discussed so far has several adverse effects for the device performance. It enhances the current density close to threshold and causes a large number of electrons to tunnel out of the upper laser level without emitting photons. In order to suppress this leakage, the QCL should be designed in such a way that the upper laser level does not extend into the collector well (#4 in Fig. 1). The simplest way to achieve this goal is to broaden the collector well since this automatically misaligns the collector well states with the laser levels. Fig. 4 (b) shows the spectral function of the QCL for a collector well width of 17.3 nm (instead of 15.5 nm, cf. Fig. 1 (b)). With this design, the collector well states lie at lower energies and the spectral density in the collector well becomes very small at the energy of the upper laser level. This modification reduces the current density around the threshold bias, as can be seen in Fig. 2 (b). In particular, the contribution of coherent tunneling to the threshold current is efficiently suppressed, as can be seen from the small ballistic current density. Our calculations show that this broadening of the collector well neither changes the peak gain energy nor the maximum value of the gain.

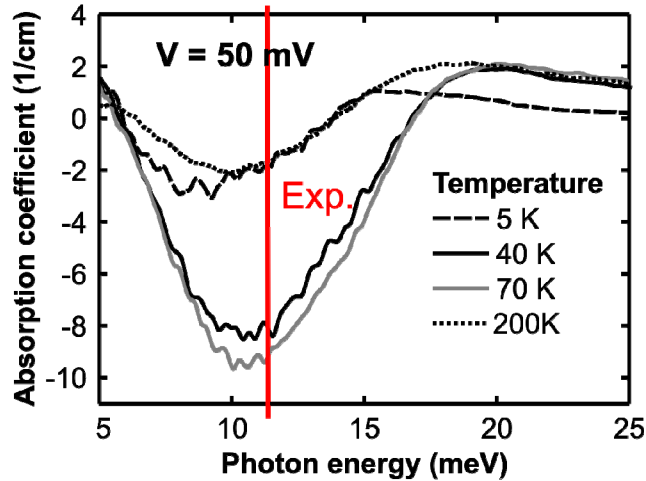


Fig. 5. Calculated absorption coefficient $\alpha(E_{\text{photon}})$ within well #2 of the QCL in Fig. 1 (a) for different temperatures. The peak gain energy agrees well with the experimental photon energy (red line).

3.4 Temperature dependence of the optical gain

In Fig. 5, we show the calculated optical absorption coefficient within well #2 of Fig. 1 (a) as a function of the photon energy and the device temperature. The peak gain energy agrees well with the experimental photon energy indicated by a vertical line in the figure. The peak optical gain reaches a maximum at a device temperature of approximately 70 K. We have already shown before [17] that higher temperatures increase the number of electrons in the upper laser level up to about 70 K. This effect causes the occupation inversion and consequently the optical gain to increase with temperature up to 70 K.

At temperatures above 70K, the amount of electrons with high in-plane kinetic energies becomes significant. This can be seen in Fig. 3 (b) that shows the energy resolved electron density in the QCL in Fig. 1 (a) at a temperature of 200 K. Here, electrons with more than 20 meV of kinetic energy above the subband minima can be found. This kinetic energy suffices for the electrons in the upper laser level ($E \sim 75$ meV in Fig. 3 (b)) to scatter into the lower laser level ($E \sim 60$ meV in Fig. 3 (b)) by emitting an optical phonon. In addition, some electrons in well #4 near $E \sim 22$ meV (see Fig. 3 (b)) can reach sufficiently high kinetic energies to fill the lower laser level. We find these mechanisms to reduce the occupation inversion and the optical gain. They are responsible for the reduction of the gain with temperatures above 70 K. Nelander and Wacker have shown [22] that there is an additional effect that limits the optical gain, the broadening of the absorption and emission linewidth namely. Since we do not take vertex corrections into account [18], the emission lines in Fig. 5 do not show such a broadening.

4. CONCLUSION

We have developed a self consistent non-equilibrium Green's function theory for stationary electron transport and optical gain in THz-QCLs. We consider the QCLs as open quantum devices. This allows one to include hot carrier effects and guarantees current conservation. Our model excellently reproduces the experimental I-V characteristics and the peak gain energy of the present THz-QCL. We find coherent and incoherent mechanisms to be equally important for the electronic transport. Our results show that thermal backfilling as well as non-radiative transitions from the upper to the lower laser level limit the maximum operating temperature. Furthermore, coherent leakage of the upper laser level turns out to efficiently contribute to the threshold current. We propose an optimized design that efficiently suppresses this coherent leakage.

5. ACKNOWLEDGEMENTS

The authors acknowledge financial support from the Deutsche Forschungsgemeinschaft (SFB 631), the Österreichische Fonds zur Förderung der Wissenschaft (SFB IRON), and the Nano Initiative Munich.

REFERENCES

- [1] Keldysh, L. P., "Diagram technique for nonequilibrium processes," Sov. Phys. JETP 20, 1018 (1965).
- [2] Kadanoff, L. P., and Baym, G., "Quantum Statistical Mechanics," Benjamin, New York, (1962).
- [3] Lake, R., Klimeck, G., Bowen, R. and Jovanovic, D., "Single and multiband modeling of quantum electron transport through layered semiconductor devices," J. Appl. Phys. 81, 7845 (1997).
- [4] Datta, S., "Electronic Transport in Mesoscopic Systems," University Press, Cambridge, (1995).
- [5] Anantram, M. P., and Govindan, T. R., "Conductance of carbon nanotubes with disorder: A numerical study, " Phys. Rev. B 58, 4882 (1998).

- [6] Cresti, A., Farchioni, R., Grosso, G., and Parravicini, G. P., "Keldysh-Green function formalism for current profiles in mesoscopic systems," *Phys. Rev. B* **68**, 075306 (2003).
- [7] Svizhenko, A., Anantram, M. P., Govindan, T. R., Biegel, B., and Venugopal, R., "Two-dimensional quantum mechanical modeling of nanotransistors," *J. Appl. Phys.* **91**, 2343 (2002).
- [8] Gagliardi, A., Solomon, G. C., Pecchia, A., Frauenheim, T., Carlo, A. D., Hush, N. S., Reimers, J. R., "A priori method for propensity rules for inelastic electron tunneling spectroscopy of single-molecule conduction," *Phys. Rev. B* **75**, 174306 (2007).
- [9] Wacker, A., *Phys. Rev. B* **66**, "Gain in quantum cascade lasers and superlattices: A quantum transport theory," 085326 (2002).
- [10] Lee, S.-C., and Wacker, A., "Nonequilibrium Green's function theory for transport and gain properties of quantum cascade structures," *Phys. Rev. B* **66**, 245314 (2002).
- [11] Vukmirović, N., Ikonić, Z., Indijin, D., and Harrison, P., "Quantum transport in semiconductor quantum dot superlattices: Electron-phonon resonances and polaron effects," *Phys. Rev. B* **76**, 245313 (2007).
- [12] Benz, A., Fasching, G., Andrews, A.M., Martl, M., Unterrainer, K., Roch, T., Schrenk, W., Golka, S., and Strasser, G., "Influence of doping on the performance of terahertz quantum-cascade lasers," *Appl. Phys. Lett.* **90**, 101107 (2007).
- [13] Nag, B. R., "Al₃Ga₇As/GaAs and Ga₅In₅P/GaAs quantum wells," *Semicond. Sci. Technol.* **19**, 162 (2004).
- [14] Unuma, T., Yoshita, M., Noda, T., Sakaki, H., and Akiyama, H., "Intersubband absorption linewidth in GaAs quantum wells due to scattering by interface roughness, phonons, alloy disorder, and impurities," *J. Appl. Phys.* **93**, 1586 (2003).
- [15] Leosson, K., Jensen, J. R., Langbein, W., and Hvam, J. M., "Exciton localization and interface roughness in growth-interrupted GaAs/AlAs quantum wells," *Phys. Rev. B* **61**, 10322 (2000).
- [16] Madelung, O., "Landolt-Börnstein, Semiconductors: Intrinsic Properties of Group IV Elements and III-V, II-VI and I-VII Compounds, Group III/22a," Springer, Berlin, (1987).
- [17] Kubis, T., Yeh, C., and Vogl, P., " Non-equilibrium quantum transport theory: Current and gain in quantum cascade lasers," *J. Comput. Electron.* **7**, 432 (2008).
- [18] Banit, F., Lee, S.-C., Knorr, A., and Wacker, A., "Self-consistent theory of the gain linewidth for quantum-cascade lasers," *Appl. Phys. Lett.* **86**, 041108 (2005).
- [19] Vitiello, M., Scamarcio, G., Spagnolo, V., Williams, B. S., Kumar, S., Hu, Q., and Reno, J. L., "Measurement of subband electronic temperatures and population inversion in THz quantum-cascade lasers," *Appl. Phys. Lett.* **86**, 111115 (2005).
- [20] Callebaut, H., Kumar, S., Williams, B. S., Hu, Q., and Reno, J. L., "Analysis of transport properties of terahertz quantum cascade lasers," *Appl. Phys. Lett.* **83**, 207 (2003).
- [21] Iotti, R. C., and Rossi, F., "Nature of Charge Transport in Quantum-Cascade Lasers," *Phys. Rev. Lett.* **87**, 146603 (2001).
- [22] Nelander, R., and Wacker, A., "Temperature dependence of the gain profile for terahertz quantum cascade lasers," *Appl. Phys. Lett.* **92**, 081102 (2008).